JOURNAL OF COMPUTATIONAL PHYSICS 107, 105–117 (1993)

Almost Poisson Integration of Rigid Body Systems*

MARK A. AUSTIN

Department of Civil Engineering and Institute for Systems Research, University of Maryland, College Park, Maryland 20742

P. S. KRISHNAPRASAD

Department of Electrical Engineering and Institute for Systems Research, University of Maryland, College Park, Maryland 20742

AND

LI-SHENG WANG

Institute of Applied Mechanics, National Taiwan University, Taipei, Taiwan, Republic of China

Received May 7, 1991

In this paper we discuss the numerical integration of Lie–Poisson systems using the mid-point rule. Since such systems result from the reduction of hamiltonian systems with symmetry by Lie group actions, we also present examples of reconstruction rules for the full dynamics. A primary motivation is to preserve in the integration process, various conserved quantities of the original dynamics. A main result of this paper is an $O(h^3)$ error estimate for the Lie–Poisson structure, where h is the integration step-size. We note that Lie–Poisson systems appear naturally in many areas of physical science and engineering, including theoretical mechanics of fluids and plasmas, satellite dynamics, and polarization dynamics. In the present paper we consider a series of progressively complicated examples related to rigid body systems. We also consider a dissipative example associated to a Lie–Poisson system. The behavior of the mid-point rule and an associated reconstruction rule is numerically explored.

1. INTRODUCTION

Natural dynamical systems often display a variety of analytic and geometric structures in their mathematical descriptions. Associated to such structures, there are various conserved quantities or invariants of analytic as well as geometric character. For instance, in hamiltonian mechanics of particles in a central force field, one has conservation of energy and total angular momentum. The phase space volume is also conserved. The latter is an example of a geometric conserved quantity. In the case of dissipative systems the volume decays. In the study of such systems via computer simulation, it is very desirable to use computational schemes that admit the same set of invariants (or decay rates). More precisely, one would like to preserve underlying geometric structures and symmetries even in the discrete-time dynamics (computational scheme), in the interest of long-term predictions. If, as is customary, one were to use off-the-shelf schemes (e.g., fourth or higher order explicit Runge–Kutta [20], backward Euler, diagonally implicit Runge–Kutta [2]) to integrate the dynamics in such problems, then the computed trajectories show systematic deviations (decay or growth) in the quantities that are physically conserved. Thus, such numerical simulations are an unreliable guide to the long-term dynamic behavior. For related comparisons, see Channel and Scovel [5].

For some time there has been steady interest in the design of algorithms that have the facility to closely mimic hamiltonian dynamics. In the work of the Beijing school [9, 10], for example, we find a systematic exploration of symplectic schemes (via generating functions) for classical hamiltonian systems on flat spaces. The mid-point rule plays a prominent role in that work. In the present paper, we are concerned with systems that evolve on cotangent bundles of Lie groups, a basic example being the free rigid body with the rotation group as configuration space. If the hamiltonian is fully reducible by the group, as is the case in the rigid body example, then the dynamics drops to the flat space of linear functionals on the Lie algebra of the Lie group, and hence the mid-point rule is well defined globally in the reduced variables. The hamiltonian structure of the reduced equations is noncanonical, and is referred to as a

* This work was supported in part by the AFSOR University Research Initiative Program under Grants AFSOR-87-0073 and AFSOR-90-0105; by the National Science Foundation's Engineering Research Centers Program, NSFD CDR 8803012; by NSF Research Initiation Grant NSF BCS 8907722; and also by the Army Research Office through the Mathematical Sciences Institute at Cornell University.

0021-9991/93 $5.00

Lie–Poisson structure. It is a principal goal of this paper to explore the applications (via a series of progressively complicated examples) of the mid-point rule and related reconstruction rules to such Lie–Poisson equations. In general, the mid-point rule is not exactly Poisson structure preserving (and hence the terminology of almost Poisson integration). However, by a small miracle involving the Jacobi identity, the mid-point rule is second-order accurate in the Poisson structure, and to this end we give an error formula.

The structure of the paper is as follows. In Section 2 we present the basic model of (noncanonical) Poisson dynamics and summarize some of its properties. We also specialize it to the classical canonical setting. In Section 3 we discuss the mid-point rule and present an error formula for the Poisson bracket. The mid-point rule is applied to a variety of examples in Section 4; these include rigid body dynamics, heavy top, and dual spin setellite with internally damped rotors. A key result is the derivation of a reconstruction formula for elements in $SO(3)$ (the rotation group), which conserves spatial angular momentum. Section 5 describes the numerical implementation of the proposed algorithms. Finally, results of numerical experiments are presented in Section 6.

A Lie–Poisson Hamilton–Jacobi theory has been formulated by Marsden and Ge-Zhong [12]. This theory leads to algorithms that preserve the Lie–Poisson structure exactly, but do not typically conserve the Hamiltonian. Recently, Simo and Wong [22] have used a Newmark-based algorithm to study rigid body dynamics. When the parameters of their algorithms are set so that energy and momentum will be conserved, their algorithm reduces to the mid-point rule, together with an exponential map. We note, however, that the work of Simo and Wong does not consider errors, from the viewpoint of conserving the Poisson structure, and has not been extended to applications with a general Lie–Poisson setting. For other earlier work on the mid-point rule, we refer the reader to Elliott [7, 8].

2. THE MODEL

In the present paper we are concerned with hamiltonian models of the form,

$$\dot{z} = \Lambda(z)\,\nabla H(z). \tag{1}$$

Here $\Lambda(z)$, the Poisson tensor, is an $n \times n$ skew-symmetric matrix for each z and H is the hamiltonian. In addition, the tensor $\Lambda(z)$ satisfies a set of differential equations (Jacobi identity):

$$\sum_l \frac{\partial \Lambda^{ij}(z)}{\partial z_l}\Lambda^{lk}(z) + \frac{\partial \Lambda^{jk}(z)}{\partial z_l}\Lambda^{li}(z) + \frac{\partial \Lambda^{ki}(z)}{\partial z_l}\Lambda^{lj}(z) = 0. \tag{2}$$

With condition (2), the operation

$$\{f, g\} = \nabla f^{\mathrm{T}}\,\Lambda(z)\,\nabla g \tag{3}$$

is a well-defined Poisson bracket on the space of smooth functions on $\mathbb{R}^n$. It is remarkable that the equations of many physical and engineering problems are based on models of the form of (1) or perturbations thereof. We note, for example, the dynamics of dual spin satellites [15], accelerator dynamics [6], motion of a heavy top [3], Euler's elastica [18], and dynamics of rods, plates, and shells [21]. Also see Simo, Marsden, and Krishnaprasad [21] for infinite-dimensional examples and Marsden *et al.* [17] for a general discussion.

The dynamics (1) can be re-expressed in terms of the Poisson bracket (3) as

$$\dot{z}_i = \{z_i, H\}. \tag{4}$$

When $\Lambda(z)$ is linear in z, the bracket structure is said to be of *Lie–Poisson type*. Several of the earlier mentioned examples are of this variety. Let

$$\Lambda^{ij}(z) = \sum_{k=1}^{n} \Gamma^k_{ij} z_k, \tag{5}$$

subject to the constraint $\Gamma^k_{ij} = -\Gamma^k_{ji}$. By substituting (5) into the Jacobi identity (2), it can be shown that

$$\sum_{l=1}^{n} \Gamma^l_{ij}\Gamma^r_{lk} + \Gamma^l_{jk}\Gamma^r_{li} + \Gamma^l_{ki}\Gamma^r_{lj} = 0, \qquad 1 \leqslant i, j, k \leqslant n. \tag{6}$$

For this particular case, it is well known that the underlying vector space $\mathbb{R}^n$ can be given the structure of a Lie algebra [24] with the structure constants Γ^k_{ij} in a suitable basis. Now let $\Phi: \mathbb{R}^n \to \mathbb{R}^n$ be a diffeomorphism. Φ is said to be a Poisson automorphism if it preserves the Poisson structure, i.e., for smooth functions f, g,

$$\{f, g\} \circ \Phi = \{f \circ \Phi, g \circ \Phi\},$$

or, alternatively, its Fréchet derivative satisfies

$$(D\Phi(z))\,\Lambda(z)(D\Phi(z))^{\mathrm{T}} = \Lambda(\Phi(z)). \tag{7}$$

Here the superscript T denotes matrix transpose. We recall the well-known result (see Weinstein [24]),

PROPOSITION 1. *The flow Φ^t of the system* (1) *satisfies*:

(a) *It is a Poisson automorphism* $\forall t$.

(b) $H(\Phi^t(z)) = H(z)$.

(c) *If C: $\mathbb{R}^n \to \mathbb{R}$ is a function such that $\Lambda(z)\,\nabla C(z) = 0$, then C yields a kinematic conservation law of* (1).

Remark 1. Functions C as in Proposition 1 are called *Casimir functions*. For canonical hamiltonian systems,

$$\Lambda(z)=\begin{bmatrix} 0 & \mathbb{1} \\ -\mathbb{1} & 0 \end{bmatrix}.$$

Here $\mathbb{1}$ denotes the identity transformation on $\mathbb{R}^m$, where $m=n/2$. The corresponding canonical Poisson bracket is

$$\{f,g\}=\sum_{i=1}^{m}\left[\frac{\partial f}{\partial q_i}\frac{\partial g}{\partial p_i}-\frac{\partial f}{\partial p_i}\frac{\partial g}{\partial q_i}\right], \tag{8}$$

where the coordinates q_i and momenta p_i together define $z=(q_1,\dots,q_m,p_1,\dots,p_m)^{\mathrm{T}}$ with $n=2m$. For canonical hamiltonian systems, Casimir functions are constants. However, in the Lie–Poisson setting, nontrivial Casimir functions are common, as will be demonstrated by our examples in Section 4.

3. THE MID-POINT RULE

A basic concern of this paper is to investigate numerical algorithms that closely mimic Proposition 1. In particular, we are interested in the mid-point rule, a scheme well known to be symplectic in the canonical case [9]. Consider the implicit recursion,

$$\left[\frac{z^{k+1}-z^k}{h}\right]=\Lambda\left(\frac{z^k+z^{k+1}}{2}\right)\nabla H\left(\frac{z^k+z^{k+1}}{2}\right). \tag{9}$$

This is a discrete analog of (1) for time-step h. It is a second-order accurate integrator, and for small enough h, defines a diffeomorphism Φ_H^h via

$$z^{k+1}=\Phi_H^h(z^k). \tag{10}$$

We compute the Fréchet derivative $D\Phi_H^h(z)$ as follows: By definition, $y=\Phi_H^h(z)$ is the unique solution to the implicit equation

$$F(z,y)\triangleq y-z-h\Lambda\left(\frac{z+y}{2}\right)\nabla H\left(\frac{z+y}{2}\right)=0. \tag{11}$$

Differentiating $F(z,\Phi_H^h(z))=0$ gives

$$D_1F+D_2F\circ D\Phi_H^h=0, \tag{12}$$

where D_iF, $i=1,2$, denote the partial Fréchet derivatives. For h small enough, D_2F has an inverse, and (12) may be rearranged to give

$$D\Phi_H^h(z)=-(D_2F)^{-1}\cdot(D_1F). \tag{13}$$

For the special case $\Lambda(z)\equiv\Lambda$ a constant, it is easy to see that

$$D_1F=-\mathbb{1}-\frac{h}{2}\Lambda H_{zz}\left(\frac{z+\Phi_H^h(z)}{2}\right)$$

and

$$D_2F=\mathbb{1}-\frac{h}{2}\Lambda H_{zz}\left(\frac{z+\Phi_H^h(z)}{2}\right).$$

Letting $Q(z)=H_{zz}((z+\Phi_H^h(z))/2)$ denote the symmetric Hessian matrix, we obtain

$$D\Phi_H^h(z)=\left[\mathbb{1}-\frac{h}{2}\Lambda Q(z)\right]^{-1}\left[\mathbb{1}+\frac{h}{2}\Lambda Q(z)\right]. \tag{14}$$

PROPOSITION 2. (Wang [23]). *If $\Lambda(z)\equiv\Lambda$ a constant, then the mid-point rule is a Poisson automorphism.*

Proof. We need to show that

$$D\Phi_H^h(z)\,\Lambda(D\Phi_H^h(z))^{\mathrm{T}}=\Lambda.$$

Based on the above calculations, this reduces to showing that

$$\left[\left(\mathbb{1}-\frac{h}{2}\Lambda Q(z)\right)^{-1}\left(\mathbb{1}+\frac{h}{2}\Lambda Q(z)\right)\right]$$
$$\times\Lambda\left[\left(\mathbb{1}-\frac{h}{2}\Lambda Q(z)\right)^{-1}\left(\mathbb{1}+\frac{h}{2}\Lambda Q(z)\right)\right]^{\mathrm{T}}=\Lambda,$$

which is equivalent to showing that

$$\left[\mathbb{1}+\frac{h}{2}\Lambda Q(z)\right]\Lambda\left[\mathbb{1}+\frac{h}{2}\Lambda Q(z)\right]^{\mathrm{T}}$$
$$=\left[\mathbb{1}-\frac{h}{2}\Lambda Q(z)\right]\Lambda\left[\mathbb{1}-\frac{h}{2}\Lambda Q(z)\right]^{\mathrm{T}}.$$

This follows from the fact that $\Lambda=-\Lambda^{\mathrm{T}}$ and $Q(z)=Q(z)^{\mathrm{T}}$. The proof is now complete.

Remark 2. It follows from the above proposition that if $\Lambda(z)\equiv\Lambda=\left[\begin{smallmatrix} 0 & \mathbb{1} \\ -\mathbb{1} & 0 \end{smallmatrix}\right]$ (i.e., we are in the canonical case), then the mid-point rule preserves the classical Poisson bracket (8). In such cases, we recover the well-known result that the mid-point rule is a symplectic integrator (Feng [10]). This result also follows from the observation that in the canonical case, formula (14) becomes a Cayley transform of an *infinitesimally symplectic matrix $\Lambda Q(z)$ and hence $D\Phi_H^h(z)$* is symplectic.

When $\Lambda(z)$ is not a constant, in general, the mid-point rule is not a Poisson automorphism. The following theorem shows that when $\Lambda(z)$ is linear in z (i.e., we are in the Lie–Poisson setting) the mid-point rule is an *almost* Poisson integrator in the sense that it preserves the Lie–Poisson structure up to second order. To this end, an error formula is given.

THEOREM 1. *For Lie–Poisson systems the mid-point rule is almost a Poisson automorphism. We have the error formula*

$$D\Phi_H^h(z)\,\Lambda(z)(D\Phi_H^h(z))^{\mathrm{T}} - \Lambda(\Phi_H^h(z)) = -\frac{h^3}{4} K(z)\,\Lambda\left(\Lambda\left(\frac{z+\Phi_H^h(z)}{2}\right) w\right) K(z)^{\mathrm{T}} + O(h^4), \quad (15)$$

where

$$K(z) = \Lambda\left(\frac{z+\Phi_H^h(z)}{2}\right) Q + \Omega(w),$$

$$Q = D^2 H\left(\frac{z+\Phi_H^h(z)}{2}\right),$$

$$w = \nabla H\left(\frac{z+\Phi_H^h(z)}{2}\right).$$

Here Q is the Hessian of H evaluated at the mid-point, and Ω is defined by requiring that $\Omega(v)\,y = \Lambda(y)v$, where $v, y \in \mathbb{R}^n$.

Proof. Recall that the partial Fréchet derivatives for $v \in \mathbb{R}^n$ are

$$D_1 F(z, y)v \triangleq \lim_{t\to 0} \frac{F(z+tv, y) - F(z, y)}{t}$$

$$D_2 F(z, y)v \triangleq \lim_{t\to 0} \frac{F(z, y+tv) - F(z, y)}{t}.$$

It can be verified that

$$D_1 F = -\left[\mathbb{1} + \frac{h}{2}\Lambda\left(\frac{z+y}{2}\right) D^2 H\left(\frac{z+y}{2}\right) + \frac{h}{2}\Omega\left(\nabla H\left(\frac{z+y}{2}\right)\right)\right] \quad (16)$$

and

$$D_2 F = \left[\mathbb{1} - \frac{h}{2}\Lambda\left(\frac{z+y}{2}\right) D^2 H\left(\frac{z+y}{2}\right) - \frac{h}{2}\Omega\left(\nabla H\left(\frac{z+y}{2}\right)\right)\right]. \quad (17)$$

In the following derivation, y in (16) and (17) will be used to denote $\Phi_H^h(z)$. The error in the Poisson structure Λ due to discrete time stepping by Φ_H^h is given by

$$\varepsilon = D\Phi_H^h(z)\,\Lambda(z)(D\Phi_H^h(z))^{\mathrm{T}} - \Lambda(\Phi_H^h(z)). \quad (18)$$

Substituting (16) and (17) into (13) gives

$$\varepsilon = (D_2 F)^{-1}(\varepsilon_1)(D_2 F)^{\mathrm{T}-1}, \quad (19)$$

where

$$\varepsilon_1 = (D_1 F)\,\Lambda(z)(D_1 F)^{\mathrm{T}} - (D_2 F)\,\Lambda(y)(D_2 F)^{\mathrm{T}}. \quad (20)$$

Since $(D_2 F)^{-1} = \mathbb{1} + O(h)$, we are mainly interested in the behavior of ε_1 as a function of h. For notational convenience, we write the mid-point $(z+\Phi_H^h(z))/2$ as x and define $\delta = y - z = \Phi_H^h(z) - z$. The terms of formula (20) are now multiplied out. By invoking (16) and (17) and noting the linearity of Λ and Ω in their respective arguments, we obtain

$$\begin{aligned}\varepsilon_1 = {} & [-\Lambda(\delta) + h\Omega(w)\,\Lambda(x) + h\Lambda(x)\,\Omega(w)^{\mathrm{T}}] \\ & + [h\Lambda(x)\,Q\Lambda(x) + h\Lambda(x)\,Q\Lambda(x)^{\mathrm{T}}] \\ & + \left[-\frac{h^2}{4}\Lambda(x)\,Q\Lambda(\delta)\,Q\Lambda(x)^{\mathrm{T}} - \frac{h^2}{4}\Omega(w)\,\Lambda(\delta)\,Q\Lambda(x)^{\mathrm{T}}\right] \\ & - \left[\frac{h^2}{4}\Lambda(x)\,Q\Lambda(\delta)\,\Omega(w)^{\mathrm{T}} + \frac{h^2}{4}\Omega(w)\,\Lambda(\delta)\,\Omega(w)^{\mathrm{T}}\right].\end{aligned} \quad (21)$$

The second square bracket in ε_1 vanishes because $\Lambda = -\Lambda^{\mathrm{T}}$. Recall from (9) that

$$\delta = h\Lambda(x)w. \quad (22)$$

After (22) is substituted into (21), we note that the first square bracket in (21) is linear in h, and when multiplied by v it takes the form

$$h[-\Lambda(\Lambda(x)w) + \Omega(w)\,\Lambda(x) + \Lambda(x)\,\Omega(w)^{\mathrm{T}}]v. \quad (23)$$

We wish to show that expression (23) also vanishes. This is equivalent to showing that

$$[-\Lambda(\Lambda(x)w) + \Omega(w)\,\Lambda(x) + \Lambda(x)\,\Omega(w)^{\mathrm{T}}]v = 0, \quad \forall v \in \mathbb{R}^n. \quad (24)$$

Recalling that the definition for Ω is given by $\Omega(v)\,y = \Lambda(y)v$, the left-hand side of (24) can be re-written as

$$-\Omega(v)\,\Lambda(x)w + \Omega(w)\,\Omega(v)x + \Lambda(x)\,\Omega(w)^{\mathrm{T}}\,v. \quad (25)$$

The next step is to expand Ω and Λ via the structure constants Γ_{ij}^k. One can then show that precisely because of the Jacobi identity (6), expression (25) vanishes for all v, w, $x \in \mathbb{R}^n$. This is the small miracle alluded to in the Introduction! Collecting together the terms in the third and fourth square brackets in formula (21) for ε_1 we obtain

$$\varepsilon_1 = -\frac{h^3}{4}[A(x)Q + \Omega(w)]\,A(A(x)w) \times [A(x)Q + \Omega(w)]^{\mathrm{T}} = -\frac{h^3}{4} K(z) A\left[A\left(\frac{z+\Phi_H^h(z)}{2}\right)w\right]K(z)^{\mathrm{T}}.$$

It follows that

$$\varepsilon = (D_2F)^{-1}(\varepsilon_1)(D_2F)^{\mathrm{T}-1} = (\mathbb{1} + O(h))^{-1}(\varepsilon_1)(\mathbb{1} + O(h))^{-1} = -\frac{h^3}{4} K(z) A\left(A\left(\frac{z+\Phi_H^h(z)}{2}\right)w\right)K(z)^{\mathrm{T}} + O(h^4).$$

This completes the proof.

Conserved Quantities of Poisson System (1)

It is well known that the mid-point rule is a second-order algorithm. Accordingly, a conserved quantity is expected to be approximated accurately up to second order. If $F(z)$ is a first integral of (1), then we have

$$\nabla F(z)^{\mathrm{T}} A(z) \nabla H(z) = 0, \qquad \forall z \in \mathbb{R}^n. \tag{26a}$$

Assuming $F(z)$ is also three times continuously differentiable, then by Taylor's theorem, we can expand F around z^k as

$$\begin{aligned} F(z^{k+1}) = {} & F(z^k) + \nabla F(z^k)^{\mathrm{T}}(z^{k+1} - z^k) \\ & + \tfrac{1}{2} D^2 F(z^k)\cdot(z^{k+1}-z^k)\cdot(z^{k+1}-z^k) \\ & + \tfrac{1}{6} D^3 F(z^k)\cdot(z^{k+1}-z^k)\cdot(z^{k+1}-z^k) \\ & \cdot(z^{k+1}-z^k) + O(\|z^{k+1}-z^k\|^4). \end{aligned} \tag{26b}$$

It can be checked that when the mid-point rule (9) is plugged into (26b),

$$F(z^{k+1}) - F(z^k) = \tfrac{1}{24} D^3 F(z^k)\cdot u \cdot u \cdot u + O(h^4), \tag{26c}$$

where

$$u = A\left(\frac{z^{k+1}+z^k}{2}\right)\nabla H\left(\frac{z^{k+1}+z^k}{2}\right).$$

Equation (26c) is an error formula for conserved quantities of (1), which contains only third or higher order terms. It follows that the mid-point rule (9) preserves exactly any conserved quantity having only linear and quadratic terms, including Casimir functions and the Hamiltonian for (1). We have the following proposition, which will be referred to later.

PROPOSITION 3. *The discrete analog* (9) *conserves all Casimir functions and the Hamiltonian H of* (1) *if they contain only linear and quadratic terms.*

In the next section, we consider a set of examples related to rigid body mechanics that captures the essence of the results of this section.

4. EXAMPLES FROM RIGID BODY MECHANICS

The noncanonical hamiltonian model of this paper—the Lie–Poisson case in particular—arises naturally in a variety of problems in rigid body mechanics. In this section, we discuss: (a) the simple rigid body, (b) the heavy top, and (c) the dual spin satellite with internally damped rotors.

4.1. Simple Rigid Body Spinning Freely in Space

Recall that the equations of motion for a simple rigid body in three dimensions take the form:

$$\dot{A} = A\hat{\Omega}, \qquad \text{where} \quad A \in SO(3) \tag{27}$$

$$I\dot{\Omega} = I\Omega \times \Omega. \tag{28}$$

Here, $A \in SO(3)$, the group of 3×3 rotation matrices, is the matrix of direction cosines for a body frame attached to the rigid body as viewed in an inertial frame; see Fig. 1. The

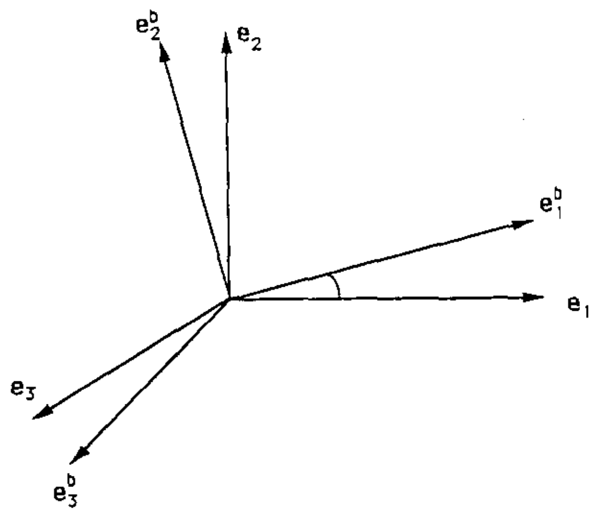

FIG. 1. Configuration of inertial and body frames.

vector Ω is the body angular velocity of the rigid body and $\hat{\Omega}$ represents a skew-symmetric matrix

$$\hat{\Omega} = \begin{bmatrix} 0 & -\Omega_3 & \Omega_2 \\ \Omega_3 & 0 & -\Omega_1 \\ -\Omega_2 & \Omega_1 & 0 \end{bmatrix}.$$

The symbol $\times$ denotes the cross-product in $\mathbb{R}^3$. Note that for an arbitrary vector y, $\hat{\Omega} y = \Omega \times y$. The matrix I denotes the moment of inertia tensor of the rigid body in the body frame. If $m = I\Omega$ denotes the body angular momentum, then we can re-write (27) and (28) as

$$\dot{A} = A\widehat{I^{-1}m} \tag{29}$$

$$\dot{m} = \hat{m} I^{-1} m. \tag{30}$$

Several observations are in order:

(a) Equation (30) is the reduction of the full dynamics (justified by the $SO(3)$-invariance of the kinetic energy) [1]. In the sense of Section 2, (30) is also Lie–Poisson, with Poisson tensor $\Lambda(m) = \hat{m}$, and hamiltonian $H(m) = \frac{1}{2} m \cdot I^{-1} m$. Hereafter $\cdot$ denotes the dot product.

(b) $C(m) = \frac{1}{2} \|m\|^2$ is a Casimir function associated to (30). It is a quadratic conserved quantity.

Our idea is to integrate (30) numerically via the mid-point rule (thereby conserving H and C, see Proposition 3), and then devise a reconstruction rule for updating the attitude matrix A in such a way that spatial angular momentum $\pi = Am$ is also conserved.

4.1.1. *Discrete Update in Body Momentum*

Let m_k and m_{k+1} be the body momentum at timesteps h_k and h_{k+1}, respectively, and $h = h_{k+1} - h_k$. The discrete update in body momentum corresponds to the mid-point rule applied to (30), i.e.,

$$\frac{m_{k+1} - m_k}{h} = \left[\frac{m_k + m_{k+1}}{2}\right] \times I^{-1} \left[\frac{m_k + m_{k+1}}{2}\right]. \tag{31}$$

Given m_k, Eqs. (31) are solved for m_{k+1}. It follows from Proposition 3 that this update scheme conserves both $H(m)$ and $C(m)$.

4.1.2. *Discrete Update in Spatial Attitude (Reconstruction Rule)*

LEMMA. *Once Eqs. (31) are solved, our reconstruction rule for the update in spatial attitude is given by the explicit set of equations*:

$$A_{k+1} = A_k[\mathbb{1} - \widehat{b_k}]^{-1} [\mathbb{1} + \widehat{b_k}] \tag{32a}$$

where

$$b_k = \left[\frac{h}{2}\right] I^{-1} \left[\frac{m_k + m_{k+1}}{2}\right]. \tag{32b}$$

Proof. The explicit recursion (32)—the Cayley Transform for $SO(3)$—is arrived at by requiring conservation of spatial angular momentum $\pi = Am$,

$$\pi_{k+1} = \pi_k = A_{k+1} m_{k+1} = A_k m_k. \tag{33a}$$

This suggests that a suitable form for the update is

$$A_{k+1} = A_k \bar{A}_k = A_k[\mathbb{1} - \widehat{b_k}]^{-1} [\mathbb{1} + \widehat{b_k}], \tag{33b}$$

where $\widehat{b_k}$ is skew-symmetric and needs to be determined so that (33b) closely approximates the matrix exponential implies by $\dot{A} = A\hat{\Omega}$. Substituting (33b) into (33a) and rearranging terms gives

$$[\widehat{m_k + m_{k+1}}]\, b_k = [m_{k+1} - m_k]. \tag{33c}$$

Note that if $[\widehat{m_k + m_{k+1}}]\, b_k = [m_{k+1} - m_k]$ has a solution, then, by the Fredholm alternative theorem,

$$\begin{aligned} (m_{k+1} - m_k) \perp \operatorname{kernel}[\widehat{m_{k+1} + m_k}]^T \\ = \operatorname{kernel}[\widehat{m_{k+1} + m_k}] \\ = \{\alpha[m_{k+1} + m_k] \mid \alpha \in \mathbb{R}\}. \end{aligned}$$

This implies that $[m_k + m_{k+1}] \cdot [m_{k+1} - m_k] = 0$, and thus conservation of Casimir is a necessary condition for conservation of spatial angular momentum. The general solution to (33c) is given by

$$b_k = \lambda_k [m_{k+1} - m_k] \times [m_{k+1} + m_k] + \alpha_k [m_{k+1} + m_k]. \tag{34}$$

How do we choose λ_k and α_k? First, note that

$$[m_{k+1} - m_k] = [\widehat{m_k + m_{k+1}}]\, b_k \tag{35a}$$

$$\begin{aligned} &= [m_k + m_{k+1}] \times b_k \\ &= [m_k + m_{k+1}] \times \lambda_k([m_{k+1} - m_k] \\ &\quad \times [m_{k+1} + m_k]) \\ &\quad + [m_k + m_{k+1}] \times \alpha_k [m_{k+1} + m_k] \end{aligned} \tag{35b}$$

$$\begin{aligned} &= [m_k + m_{k+1}] \times (\lambda_k [m_{k+1} - m_k] \\ &\quad \times [m_{k+1} + m_k]) \end{aligned} \tag{35c}$$

$$= \lambda_k \|m_k + m_{k+1}\|^2 [m_{k+1} - m_k]. \tag{35d}$$

This implies

$$\lambda_k = \frac{1}{\|m_k + m_{k+1}\|^2}. \tag{36}$$

To get $\alpha_k \neq 0$, the discrete update for body momentum (31) is substituted into (34). Rearranging terms and selecting

$$\alpha_k = \left[\frac{h}{4}\right] \cdot \frac{[m_k + m_{k+1}] \cdot I^{-1}[m_k + m_{k+1}]}{\|m_k + m_{k+1}\|^2} \tag{37a}$$

gives

$$b_k = \left[\frac{h}{2}\right] I^{-1} \left[\frac{m_k + m_{k+1}}{2}\right]. \tag{37b}$$

Remark 3. Note that the matrix product

$$[\mathbb{1} - \widehat{b_k}]^{-1} [\mathbb{1} + \widehat{b_k}]$$

$$= \exp\left[hI^{-1}\left(\widehat{\frac{m_k + m_{k+1}}{2}}\right)\right] + O(h^3). \tag{38a}$$

In fact, if $I^{-1}m$ in (29) is a constant vector across the timestep, then the incremental rule for the attitude matrix becomes

$$A_{k+1} = A_k \exp(\widehat{hI^{-1}m}). \tag{38b}$$

Thus, the update rule (33b) can be intuitively thought of as the composition of two steps. First, the angular momentum in (29) is approximated by an intermediate value. Second, the exponential in (38b) is approximated in terms of b_k by the formula (38a).

4.2. Heavy Top

Consider the motion of a rigid body fixed at a stationary point subject to the action of a uniform gravitational field, as shown in Fig. 2. If the body frame is fixed at a point O, then we define the unit vector from O to the center of mass in the body frame as χ. The spatial inertial frame is also at O with the vector $\mathbf{k}$ being one of its axes. Note that the body is acted on by a gravitational force $-Mg\mathbf{k}$, where M is the mass of the rigid body, and g is the constant of acceleration due to gravity. The kinematics of the body frame relative to the inertial frame are governed by

$$\dot{A} = A\hat{\Omega}, \quad \text{where} \quad A \in SO(3). \tag{39}$$

Moreover, if $v = A^{\mathrm{T}} \cdot \mathbf{k}$, then the equations of motion for the heavy top can be expressed as

$$\dot{m} = m \times I^{-1}m + Mglv \times \chi \tag{40a}$$

$$\dot{v} = v \times I^{-1}m, \tag{40b}$$

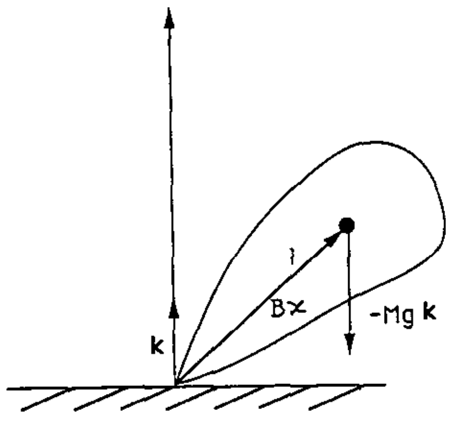

FIG. 2. Diagram for heavy top.

where $m = I\Omega$ is body momentum, l is the distance between O and the body center of mass, and I is the moment of inertia of the heavy top relative to the body frame. The heavy top conserves total energy and has two casimirs, $C_1(m, v) = \frac{1}{2}\|v\|^2$ and $C_2(m, v) = m \cdot v$; for details, see Marsden, Ratiu, and Weinstein [16]. The discrete approximation of equations (40), using the mid-point rule, is given by

$$\frac{m_{k+1} - m_k}{h} = \left[\frac{m_k + m_{k+1}}{2}\right] \times I^{-1} \frac{m_k + m_{k+1}}{2}$$

$$+ Mgl \frac{v_k + v_{k+1}}{2} \times \chi \tag{41a}$$

$$\frac{v_{k+1} - v_k}{h} = \left[\frac{v_k + v_{k+1}}{2}\right] \times I^{-1} \frac{m_k + m_{k+1}}{2}. \tag{41b}$$

It is important to note that Eqs. (41) conserve both Casimir functions and the Hamiltonian $H(m, v) = \frac{1}{2}m \cdot I^{-1}m + Mglv \cdot \chi$. This is to be expected from Proposition 3. The discrete update for the attitude matrix A of the heavy top is given by Eqs. (32).

4.3. Dual Spin Satellite with Damped Rotors

Dual spin satellites consist of a rigid body platform and several internal rotors, as shown in Fig. 3. When the platform is fully operational, the rotors are set to spin at a constant angular velocity relative to the platform. Damping rotors act as dissipators of energy. Indeed, even in the presence of mild disturbances, the transfer of momentum from the platform to the damping rotors will result in a mechanism for attitude aquisition of the platform. The spacecraft angular velocity will align itself with the rotor axis; see [15].

The equations of motion for a dual spin satellite with damping are composed of two parts. As with the two previous examples, the kinematics are given by

$$\dot{A} = A\hat{\Omega} \quad \text{where} \quad A \in SO(3). \tag{42}$$

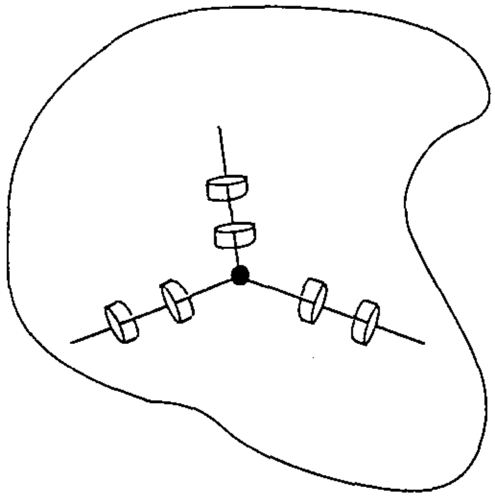

FIG. 3. Schematic of dual spin satellite with damping.

Let the diagonal matrix $\alpha = \text{diag}(\alpha_1, \alpha_2, \alpha_3)$, where $\alpha_i > 0$, and let $I_d = \text{diag}(I_d^1, I_d^2, I_d^3)$ be a diagonal matrix of moments of inertia of the damping rotors with respect to their spin axes. Note that $I_d^i \geq 0$ for $i = 1, 2, 3$. If l is the fixed internal angular momentum of the rotors, d is a momentum vector associated to damping rotors, and m is as previously defined, then the evolution of body angular momentum is governed by the equations

$$\dot{m} = (m + l + d) \times I^{-1}m - \gamma m + \delta d \tag{43a}$$

$$\dot{d} = \gamma m - \delta d, \tag{43b}$$

where $\gamma = \alpha I^{-1}$ and $\delta = \alpha I_d^{-1}$, respectively. Although the system is not a hamiltonian system in the form of (1), we still have the following properties:

(a) This system has one conserved quantity $C(m, d) = \|m + l + d\|^2$.

(b) The Lyapunov function for dual spin with damping is

$$V(m, d) = \tfrac{1}{2} m \cdot I^{-1} m + \tfrac{1}{2} d \cdot I_d^{-1} d. \tag{44a}$$

It is decrescent with

$$\dot{V} = -(I_d^{-1}d - I^{-1}m)^{\mathrm{T}} \alpha (I_d^{-1}d - I^{-1}m), \tag{44b}$$

along trajectories of (43). For details, see [15].

(c) The spatial angular momentum $\pi = A[m + l + d]$ is also a conserved quantity.

The update in body momentum is given by the mid-point rule

$$\frac{m_{k+1} - m_k}{h} = \left[\frac{m_k + m_{k+1}}{2} + l + \frac{d_k + d_{k+1}}{2}\right] \times I^{-1}\left[\frac{m_k + m_{k+1}}{2}\right] - \gamma\left[\frac{m_k + m_{k+1}}{2}\right] + \delta\left[\frac{d_k + d_{k+1}}{2}\right] \tag{45a}$$

$$\frac{d_{k+1} - d_k}{h} = \gamma\left[\frac{m_k + m_{k+1}}{2}\right] - \delta\left[\frac{d_k + d_{k+1}}{2}\right]. \tag{45b}$$

The discrete update for spatial attitude is again given by Eqs. (32). Following the steps in Section 4.1 it is easy to verify that the attitude update is momentum conserving. Indeed, techniques for reorienting the attitude of a satellite depend on a mechanism for transferring the balance of internal rotor and platform momenta, without affecting spatial angular momentum.

5. NUMERICAL INTEGRATION SCHEMES

The solution procedure for each of the applications described in Sections (4.1) through to (4.3) is: (a) solve the implicit equations for the body momentum at timestep t_{k+1}; (b) solve the explicit equations for the update in spatial attitude.

Update in body momentum. Equations (31), (41), and (45) are systems of nonlinear ordinary algebraic equations (in vector form) that must be solved at each timestep for m_{k+1}. Each equation is written in component form—let the ith component be given by $m_{[k+1,i]}$—and is rearranged so that solving the problem is equivalent to finding the roots of a system of equations, i.e., $g_i(m_k, m_{k+1}) = 0$. This gives six equations for dual spin with damping and heavy top applications, and three equations for rigid body. A damped Newton–Raphson procedure is used to solve the component equations at each timestep. If m_{k+1}^p is the pth iterate of body momentum at timestep $k+1$, then the equations to be solved at each iterate are obtaining by expanding $g_1(m_k, m_{k+1}^p)$, $g_2(m_k, m_{k+1}^p)$, and $g_3(m_k, m_{k+1}^p)$ in a Taylor series about m_{k+1}^p, truncating all second-order and higher terms, and solving the set of equations

$$\begin{bmatrix} \dfrac{\partial g_1}{\partial m_{[k+1,1]}^p} & \dfrac{\partial g_1}{\partial m_{[k+1,2]}^p} & \dfrac{\partial g_1}{\partial m_{[k+1,3]}^p} \\ \dfrac{\partial g_2}{\partial m_{[k+1,1]}^p} & \dfrac{\partial g_2}{\partial m_{[k+1,2]}^p} & \dfrac{\partial g_2}{\partial m_{[k+1,3]}^p} \\ \dfrac{\partial g_3}{\partial m_{[k+1,1]}^p} & \dfrac{\partial g_3}{\partial m_{[k+1,2]}^p} & \dfrac{\partial g_3}{\partial m_{[k+1,3]}^p} \end{bmatrix} \times \begin{bmatrix} \Delta m_{[k,1]}^p \\ \Delta m_{[k,2]}^p \\ \Delta m_{[k,3]}^p \end{bmatrix} = -\begin{bmatrix} g_1(m_k, m_{k+1}^p) \\ g_2(m_k, m_{k+1}^p) \\ g_3(m_k, m_{k+1}^p) \end{bmatrix} \tag{46}$$

for the incremental update $m^{p+1}_{[k+1,i]} = m^p_{[k+1,i]} + \Delta m^p_{[k,i]}$, where $i = 1, 2, 3$. Equations (46) may be stated more concisely $\mathbf{J} \cdot \mathbf{h} = -\mathbf{g}$. *Iterations continue at each timestep until:* (a) a preset maximum number of iterations is reached, or (b) all changes in body momentum components from (46) are less than a preset error value times the magnitude of momentum component at the beginning of the iterations. Divergence of the iterates is avoided by ensuring that $\|g(m_k, m^{p+1}_{k+1})\|_2$ is less than $\|g(m_k, m^p_{k+1})\|_2$. When this test fails, $\mathbf{h}$ is divided by powers of two until the norm of the new $[p+1]$th iterate is less than $\|g(m_k, m^p_{k+1})\|_2$.

Update in attitude. Because it is undesirable to compute matrix inverses, solutions to (32a) are obtained by first solving $[\mathbb{1} - \widehat{b_k}][x_k] = [\mathbb{1} + \widehat{b_k}]$ for the (3×3) matrix $[x_k]$, followed by the explicit update $A_{k+1} = A_k \cdot [x_k]$.

6. NUMERICAL EXPERIMENTS

Results of numerical experiments are presented for two applications: (a) motion of a rigid body spinning freely in space, and (b) dynamics of a dual spin satellite platform containing rapidly spinning internally damped rotors. In each case we are interested in verifying that simulations of the discrete dynamics match the theoretical predictions of Section 4.

6.1. EXAMPLE 1 (rigid body motion). Consider the motion of a rigid body having principal moments of inertia $I = \text{diag}(1, 2, 3)$. Initially (at time $t = 0$) the rigid body is spinning freely about its intermediate (unstable) axis with angular velocity $w = [1, 10, 1]$; 400 timesteps at $\Delta t = 0.05$ s are computed. At each timestep, iterations to solve the *equations of motion for body momentum* m_{k+1} *continue* until the magnitude of the incremental updates in angular momentum components, given by Eq. (46), are all less than $\frac{1}{100}$ of the component magnitudes for load vector $\mathbf{g}$ at the beginning of the iterations.

Energy and Casimir conservation. Figure 4 shows the time variation in energy $H(m_{k+1}) = \frac{1}{2} m_{k+1} \cdot I^{-1} m_{k+1}$ and Casimir $C(m_{k+1}) = \frac{1}{2} \|m_{k+1}\|^2$ for the rigid body. Both quantities are conserved to machine precision.

Spatial attitude. Figures 5 and 6 show the time variation in attitude matrix component $A(1,1)$ for 400 steps of simulation at $\Delta t = 0.05$ s and 4000 steps of simulation at $\Delta t = 0.005$ s, respectively. We recall that the role of the attitude matrix A is to describe the rotational orientation of the body frame relative to an inertial frame. As such, the time variation in all components of A is bounded by the interval $[-1, 1]$. Figures 5 and 6 match this observation. Our initial numerical experiments were with timestep $\Delta t = 0.05$. Although the Casimir and energy were conserved to machine precision, we suspected the validity of the sharp points in the plot of $A(1,1)$ in Fig. 5. To ensure that this was not an error in coding (it happens!) the simulations were repeated for the same time interval using $\Delta t = 0.005$ s. The results are plotted in Fig. 6. It is easy to see that time variations in peak values of attitude component $A(1,1)$ of Fig. 6 are much smoother than Fig. 5. However, the dramatic contraction in the period of the attitude components by merely decreasing the step length was not anticipated a priori. This

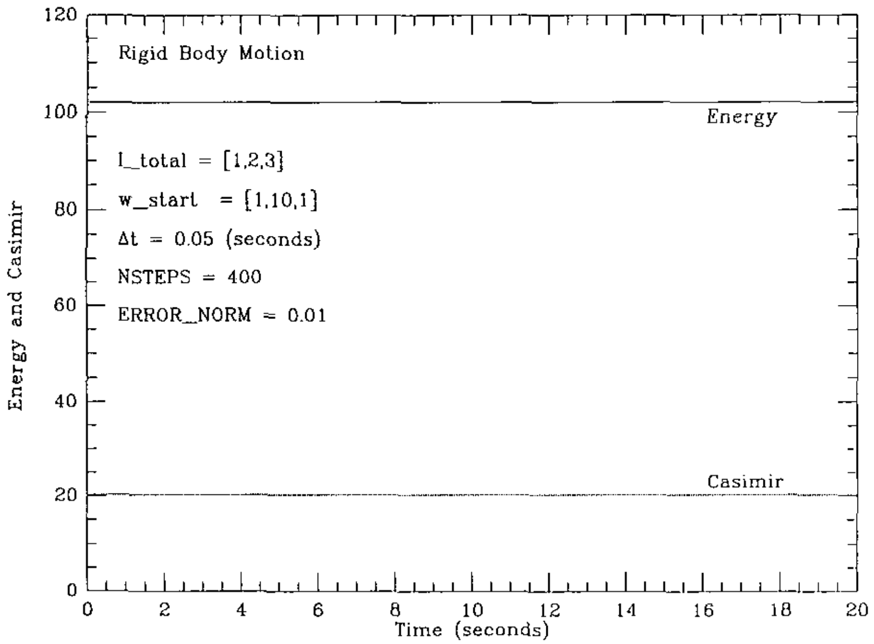

FIG. 4. Energy and Casimir for rigid body.

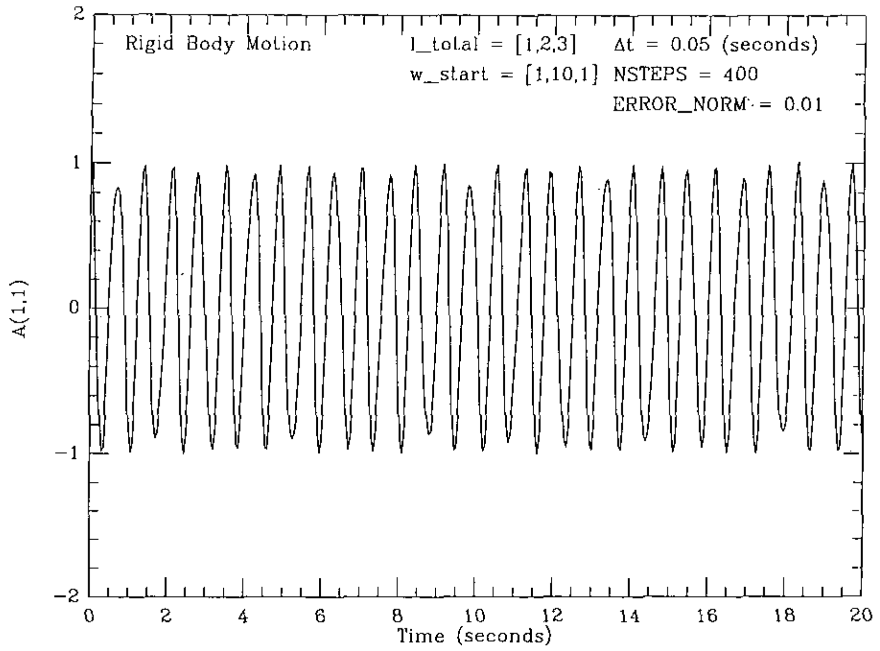

FIG. 5. $A(1, 1)$ vs time with $\Delta t = 0.05$ s.

can be seen by counting the number of cycles of $A(1, 1)$ over $t \in [0, 20]$ seconds for Figs. 5 and 6. The former has approximately 28.5 cycles, and Fig. 6 had approximately 29.3 cycles. We note that this observation is consistent with period extensions in the Newmark method; for a discussion, see Chapter 9 of Hughes [14]. Unfortunately, this observation also exposes the main weakness of the numerical approximation. While Casimir functions and energy are conserved to machine precision (indicating that the discrete dynamics follow the true trajectories in reduced phase space), we know from Section 2 that the mid-point rule is only second-order accurate in computing the Poisson bracket. This apparently translates to a systematic deviation of the discrete attitude from time-varying attitude of the

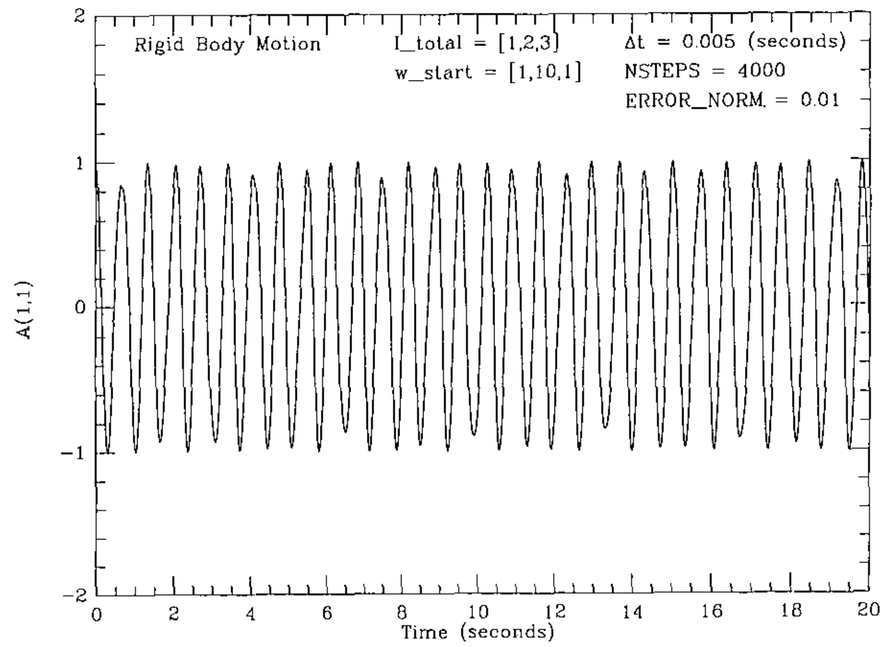

FIG. 6. $A(1, 1)$ vs time with $\Delta t = 0.005$ s.

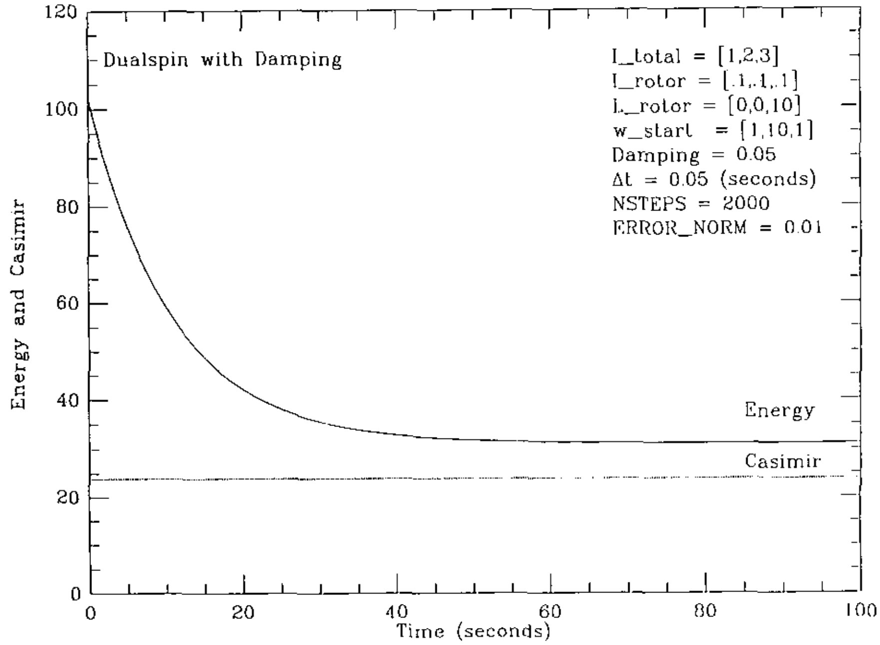

FIG. 7. Energy and conserved quantities vs time for dual spin with damping.

continuous system. Work is currently underway to try and improve the attitude prediction by combining the mid-point rule with Richardson's extrapolation techniques [4].

6.2. EXAMPLE 2 (Dual spin with damping). Our second example examines the discrete time response of a dual spin satellite platform containing three internal rotors spinning at constant angular velocity relative to the satellite platform. Principal moments of inertia for the rotors are $I_d = \text{diag}(0.1, 0.1, 0.1)$. After the rotors are locked, the combined rotors plus satellite platform is assumed to have principal moments of inertia $I = \text{diag}(1, 2, 3)$. The internal rotor is spinning with angular momentum components $L = [0, 0, 10]$. At time $t = 0$, the rigid body is spinning freely about its intermediate (unstable) axis with angular velocity $w = [1, 10, 1]$; 2000 timesteps at $\Delta t = 0.05$ s are computed.

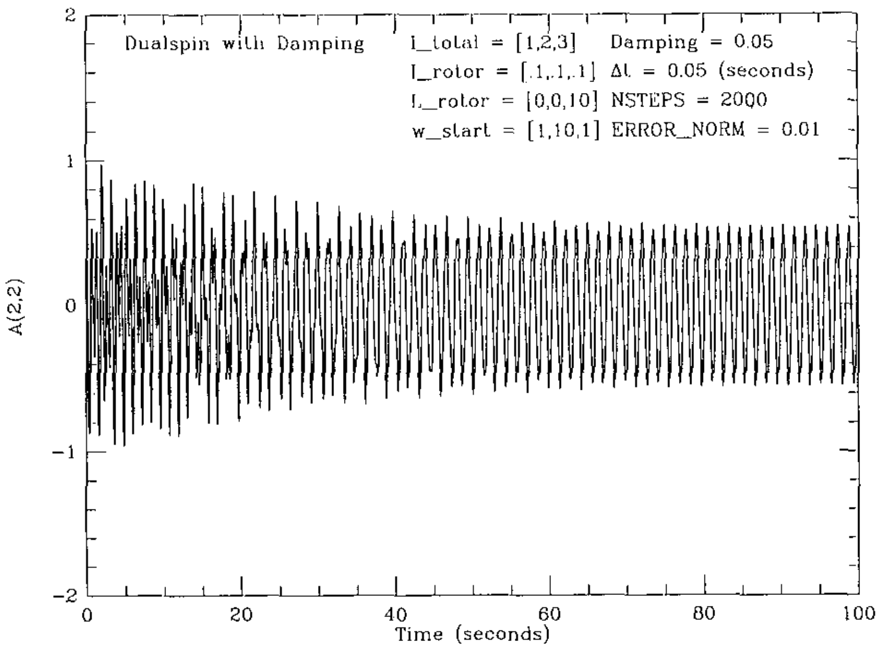

FIG. 8. $A(2, 2)$ vs time with $\Delta t = 0.05$ s.

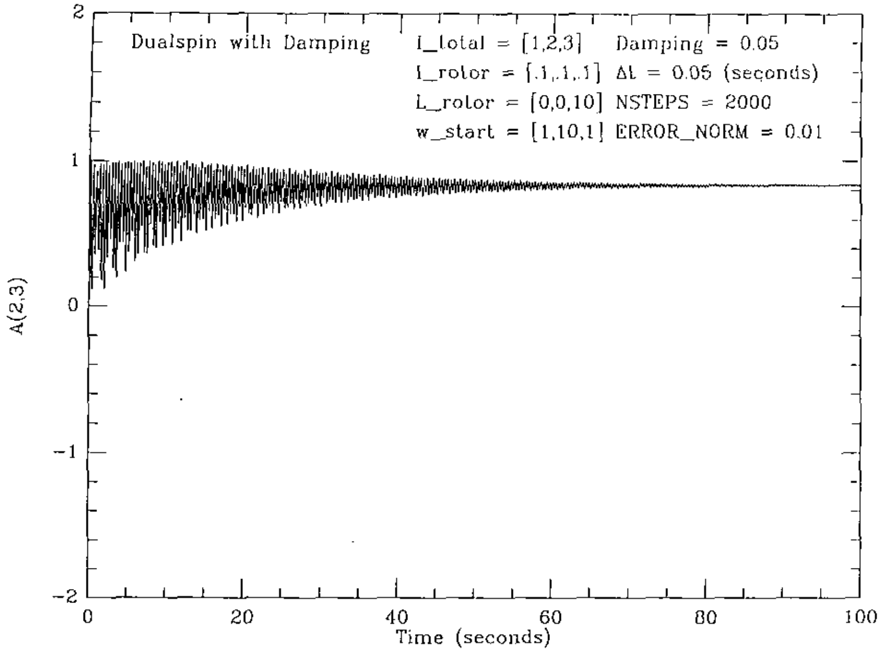

FIG. 9. $A(2, 3)$ vs time with $\Delta t = 0.05$ s.

Conserved quantities. Our discrete approximation to the Lyapunov function given in Eq. (44a) asymptotically approaches a non-zero value as theoretically predicted. At the same time, the Casimir $C(m_{k+1}, d_{k+1}) = \|m_{k+1} + l + d_{k+1}\|^2$ is conserved to machine precision (see Fig. 7).

Spatial attitude. Our numerical experiments conserve spatial angular momentum $\pi_{k+1} = A[m_{k+1} + l + d_{k+1}]$ to machine precision. As mentioned in Section 4.3, momentum transfer relies on the conservation of this quantity, and an alignment of the platform attitude along a single axis follows for high enough speeds of the driven rotors. Time variations in components of the attitude matrix $A(2, 2)$ and $A(2, 3)$ are shown in Fig. 8 and 9, respectively. Although the platform is initially tumbling in an erratic manner, the effect of damping is an alignment of the rotation about a single axis. This is inferred from component $A(2, 3)$ asymptotically approaching a single value, while component $A(2, 2)$ appears to approach a steady oscillatory motion.

7. CONCLUSIONS

Exact solutions to the flow of a Poisson system correspond to a continuous succession of Poisson automorphisms [24], and conserve all Casimirs and the Hamiltonian (when applicable). This work has been motivated by a need to find discrete approximations to the flow that have the same properties. In particular, we have focussed on the numerical integration of Lie–Poisson systems using the mid-point rule. We have proved that the mid-point rule preserves the Poisson structure up to second-order accuracy. An explicit error formula has been derived and may be used in measuring the deviations of the Poisson structure through the approximated flow. Moreover, we have shown that any naturally conserved quantity can be approximated up to second order by using the mid-point rule. For conserved quantities containing only linear and quadratic terms, such as those in the examples of this paper, the associated conservation laws are exactly satisfied.

Three rigid body systems have been studied. In each case, the dynamics in full phase space are obtained via an explicit reconstruction rule. The result is conservation of spatial angular momentum for the rigid body and dual spin satellites, and conservation of momentum along the vertical axis for the heavy top example. Future applications of study will include the approximations of the motion of a satellite in a central gravitational field and optimal control. Work is currently underway to try and improve the attitude prediction by combining the mid-point rule with Richardson's extrapolation techniques [4]. In the long term, we share the view of Simo and Wong [22] that approximation procedures for the dynamics on $SO(3)$ are directly applicable to transient dynamic calculations of geometrically exact rods and shells.

REFERENCES

1. R. Abraham and J. E. Marsden, *Foundations of Mechanics*, 2nd ed., (Benjamin/Cummings, Reading, 1978).

2. R. Alexander, *SIAM J. Numer. Methods* **14**, No. 6 (1977).

3. V. I. Arnold, *Mathematical Methods of Classical Mechanics*, Graduate Texts in Math. No. 60 (Springer-Verlag, New York, 1978).
4. M. A. Austin, *Int. J. Numer. Methods Eng.* (1993), in press.
5. P. J. Channel and C. Scovel, *Nonlinearity* **3**, 231 (1990).
6. P. J. Channel, Los Alamos National Laboratory Internal Report AT-6: ATN-86-6, 1986 (unpublished).
7. D. Elliott, in *Proceedings, First International Conference on Systems, Washington, 1987*, edited by N. DeClaris, (Optimization Software, Inc., New York, 1987).
8. D. Elliott, in *Proceedings, 29th IEEE CDC, Honolulu, Dec. '90 (IEEE, New York*, 1991), p. 1908.
9. K. Feng, in *Proceedings, 10th Intl. Conf. Numerical Methods in Fluid Mechanics, Beijing, 1986* Lecture Notes in Physics, (Springer-Verlag, New York/Berlin, 1986).
10. K. Feng, Lecture Notes in Numerical Methods for P.D.E's (Springer-Verlag, New York/Berlin, 1987).
11. Goldstein, *Classical Mechanics*, 2nd ed. (McGraw–Hill, New York, 1980).
12. Ge-Zhong and J. Mardsden, *Phys. Lett. A.* **133**, 134 (1989).
13. P. J. Holmes and J. E. Marsden, *Indiana Univ. Math. J.* **32**, No. 2 (1983).
14. T. J. R. Hughes, *The Finite Element Method: Linear Static and Dynamic Finite Element Analysis* (Prentice-Hall, Englewood Cliffs, NJ, 1987), p. 803.
15. P. S. Krishnaprasad, *Nonlinear Anal. Theory Methods Appl.* **9** (10), 1011 (1985).
16. J. E. Marsden, T. Ratiu, and A. Weinstein, "Reduction and Hamiltonian Structures on Duals of Semidirect Product Lie Algebras," in *Fluids and Plasmas: Geometry and Dynamics*, edited by J. E. Marsden, Contemporary Mathematics, Vol. 28 (Amer. Math. Soc., Providence, 1984), p. 55.
17. J. E. Marsden, O. R. O'Reilly, F. J. Wicklin, and B. W. Zombro, *Nonlinear Sci. Today* **1**(1), 4 (1991).
18. A. Mielke and P. Holmes, *Arch. Rat. Mech. Anal.* (1988).
19. J. M. Sanz-Serna, *BIT* **28**, 877 (1988).
20. A. Sela, Technical Report SRC-TR 89-7, Systems Research Center, University of Maryland, MD, 1989.
21. J. C. Simo, J. E. Marsden, and P. S. Krishnaprasad, *Arch. Rat. Mech. Anal.* **104** (2), 125.
22. J. Simo and K. K. Wong, *Int. J. Numer. Methods Eng.* **31**, 19 (1991).
23. D. L. Wang, "Symplectic Difference Schemes for Hamiltonian Systems on Poisson Manifolds," Computing Center, Academia Sinica, Beijing, China.
24. A. Weinstein, *J. Diff. Geom.* **18**, 523 (1983); **22**, 225 (1985).